

HIGH-SPEED PHOTOGRAPHY OF PYROTECHNIC MATERIALS  
AND COMPONENTS WITH A COPPER VAPOR LASER

Larry R. Dosser, John W. Reed, and Margaret A. Stark

Monsanto Research Corporation

Mound

Miamisburg, Ohio 45342\*

This document is  
**PUBLICLY RELEASABLE**

*Henry J. Keay*  
\_\_\_\_\_  
Authorizing Official

Date: 6-22-89

ABSTRACT

The evaluation of the properties of energetic materials, such as burn rate and ignition energy, is of primary importance in understanding their reactions and the functioning of devices containing them. One method for recording such information is high-speed photography at rates of up to 20,000 images per second. When a copper vapor laser is synchronized with the camera, laser-illuminated images can be recorded that detail the performance of a material or component in a manner never before possible. Recent results from high-speed photography of several pyrotechnic materials and devices will be presented. These include a pyrotechnic torch, laser ignition of high explosives, and a functioning igniter. Equilibrium chemical computations have recently been begun on the pyrotechnic torch to obtain flame compositions and temperatures. The results of these calculations, and their explanation of the change in torch function with composition, will be discussed.

INTRODUCTION

The evaluation of the properties of energetic materials, such as burn rate and ignition, is of primary importance in understanding their reactions and how devices containing them perform their function. We have

\*Mound is operated by Monsanto Research Corporation for the U.S. Department of Energy under Contract No. DE-AC04-76DP00053.

recently applied high-speed photography at rates of up to 20,000 images per second to this problem. When a copper vapor laser is synchronized to the high-speed camera, laser-illuminated images can be recorded that detail the performance of a component in a manner never before possible. The copper vapor laser used for these experiments had an average power of 30 watts, and produced pulses at a rate of up to 10 kHz. The 30 nanosecond pulselwidth of the laser essentially freezes all motion in the functioning component, thus providing stop-action pictures at a rate of up to 10,000 per second. Each laser pulse has a peak power of approximately 170,000 watts, which provides ample illumination for the high-speed photography. Several energetic materials and components have been studied with this technique, and the high-speed films will be shown in this conference. The materials and components shown will include a pyrotechnic torch, laser ignition of high explosives, and functioning pyrotechnic igniters.

#### EXPERIMENTAL

The experimental configuration used to record the high speed photographs of the energetic materials and components is shown in Figure 1. Modifications to the area labeled "Optics" are made depending on the experiment and the information sought. A typical arrangement that compresses the laser beam into a sheet to illuminate the area above a functioning component is shown in Figure 2. The laser sheet is formed with a spherical-cylindrical lens combination. The focal lengths of the two lenses are chosen to form the desired height of the sheet and to focus it at the appropriate point. After the laser sheet passes across the component, a portion of it is captured with a right angle prism and folded back around to illuminate the functioning component. The sheet lighting is a particularly useful technique for filming functioning components. When the laser sheet is passed over the center of the component, the light scattering from the smoke and particulates in the flame provides a cross-sectional view of the inside of the flame. During an experiment, the camera drives the laser with an appropriate delay that is set to a

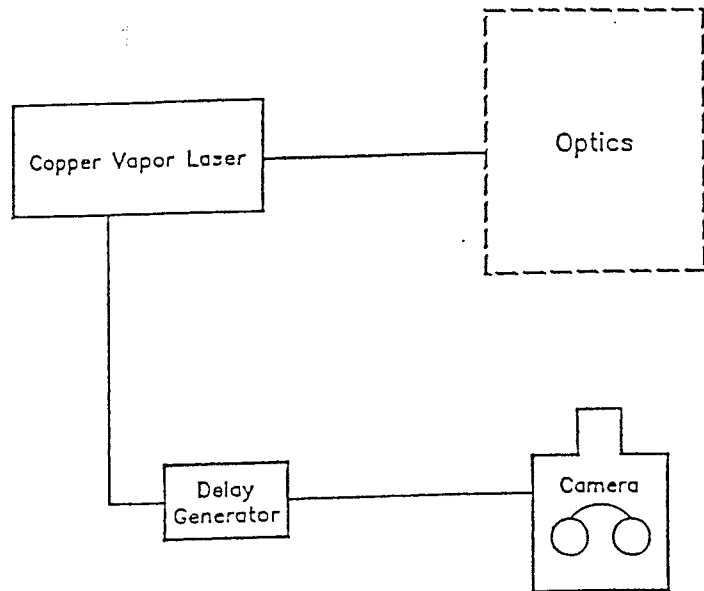


Figure 1. Experimental configuration

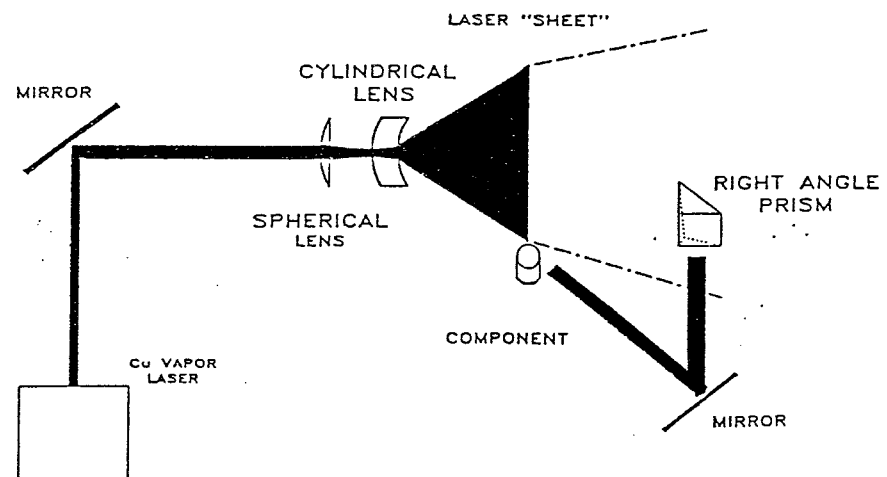


Figure 2. Optics for sheet lighting

predetermined value depending on the camera speed. This ensures that when the laser pulse is at the experimental point, the camera shutter is open and the laser-illuminated image is recorded. The shutter is open for only a few microseconds, so the timing must be quite precise. The choice of camera lens, filters, film speed, and f stop are dictated by the experiment. For most experiments, unless there is an uncommon amount of self-illumination from the material or component, the f stop is set wide open. The camera is a rotating prism camera that provides one trigger pulse per frame. When an eight-sided prism is used in this camera, full frame images are recorded. For this work a sixteen-sided prism was used, and two images were recorded per frame. Since there is only one trigger pulse per frame, one of these images is illuminated with a laser pulse, the other is not. This provides a direct comparison between laser and nonlaser-illuminated images and clearly shows the usefulness of the laser for this type of photography.

### RESULTS

The results from several different types of experiments are shown on the accompanying videotape. The high-speed films were transferred to the videotape by a special process, allowing us to examine the experiments one image at a time without excessive wear on the original film.

The pyrotechnic torch was filmed at a rate of 8 kHz, because of the high speed at which the torch functioned. The sheet lighting through the torch flame clearly showed the internal structure of the flame during the initial stages of ignition. A photograph of the tenth frame of torch burn is shown in Figure 3. The laser illumination clearly showed the differences between hot and cold particles that were emitted from the torch. The cold particles, or unburned solids, were green from the scattered laser light. The hot particles appeared white to yellow depending on their temperature.

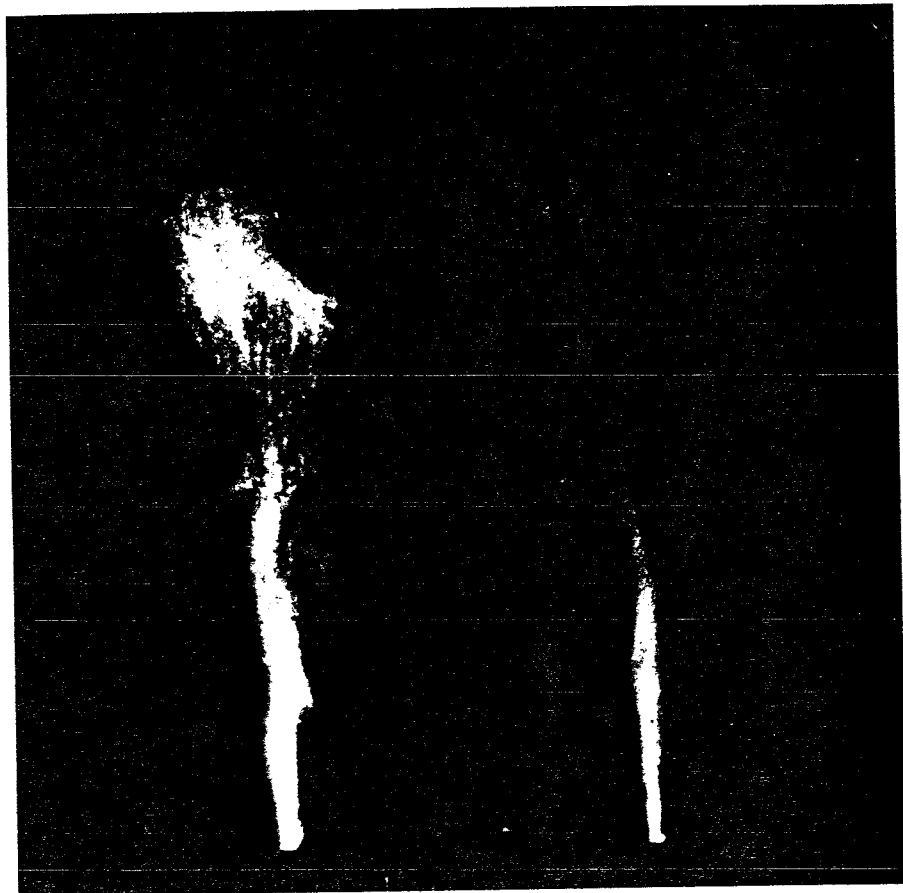


Figure 3. Pyrotechnic torch flame. Left image is laser-illuminated.

In an attempt to gain insight into the processes causing the effects observed with the modified torch, equilibrium chemical computations were made to obtain flame compositions, temperatures and associated pressures. These computations were made using the NASA Lewis Chemical Equilibrium Code (Ref. 1). The two most significant observations were the flame oscillations and the buildup of solids at the nozzle. The fuel in the torch consists of a small amount of ignition mix (B/CaCrO<sub>4</sub>), a transfer pellet made up of magnesium, C-H-F compounds and red lead oxide and an output pellet made up of aluminum, potassium perchlorate, nickel oxide and C-H-F compounds. The compositions are shown in Table 1.

Table 1  
TORCH COMPOSITION

Transfer Mix		Output Mix	
	%		%
Magnesium	45	Aluminum	24
Halon	22.	KC <sub>1</sub> O <sub>4</sub>	32
Red Lead	12.09	NiO <sub>1.2</sub>	32
Fluorel	3.75	Fluorel	6
		Halon	6

The modifications consist of the addition of 7% each of silicon and cupric oxide to the transfer mix. Flame temperatures obtained from the equilibrium computations for the output mix are shown in Figure 4 where the flame temperatures are plotted against Oxidizer-Fuel ratios (O/F). Aluminum is considered the fuel while the remaining materials are considered oxidizer. The O/F ratio as used is 2.66 and ratios on either side are plotted to show the effect of compositional changes. The temperature at O/F ratio 2.66 is 3750 K. The maximum flame temperature is not obtained at this ratio but at about O/F = 4.0 where the temperature is about 4060 K. It is assumed that the transfer mix contributes to the overall process but not completely. It is not known how much transfer mix is consumed during the reaction process. There is often some transfer pellet remaining after reaction. The effect of adding transfer mix to the output process is to lower the flame temperature. This effect is shown in

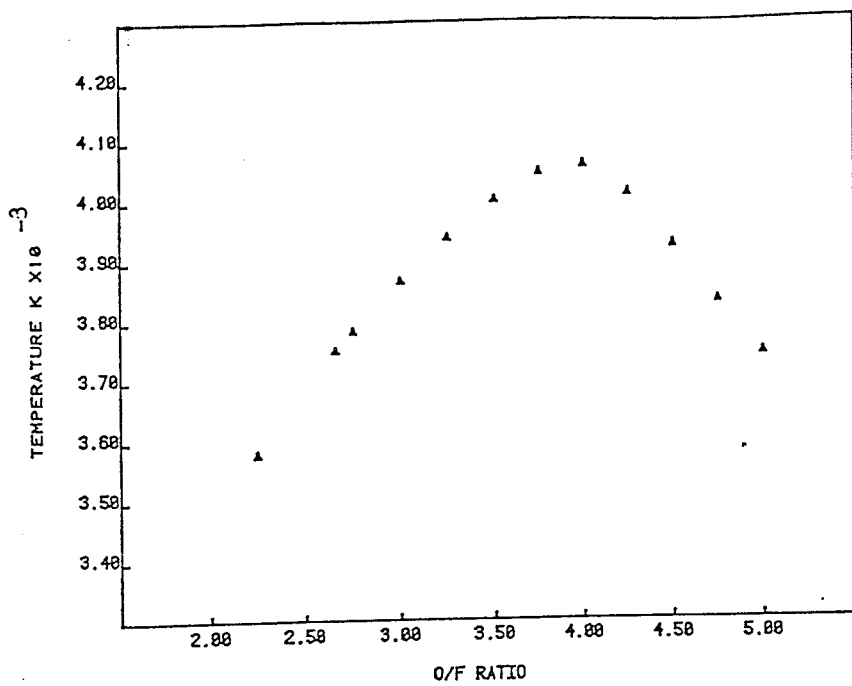


Figure 4. Output pellet stoichiometry and temperature

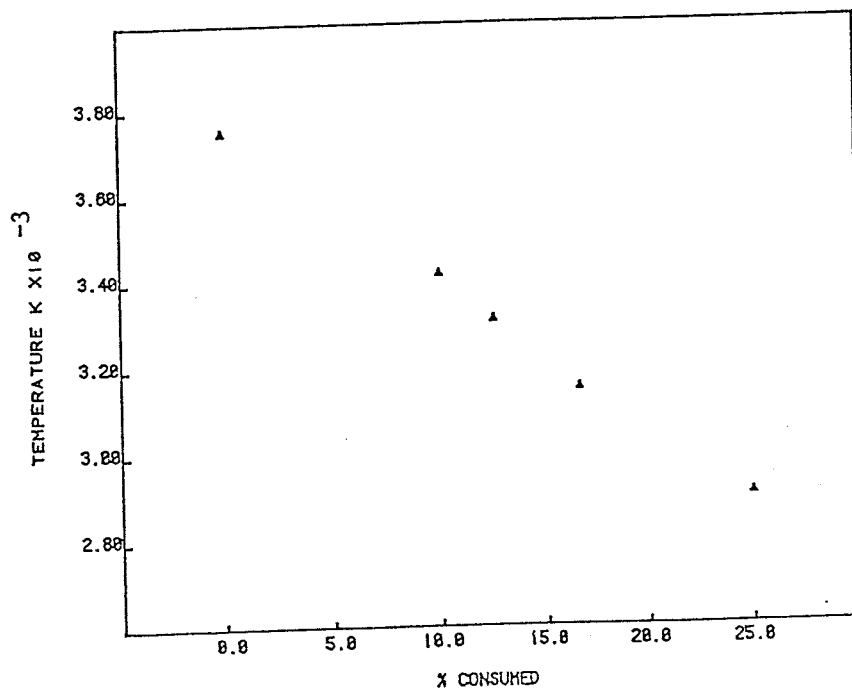


Figure 5. Temperature and % transfer composition consumed

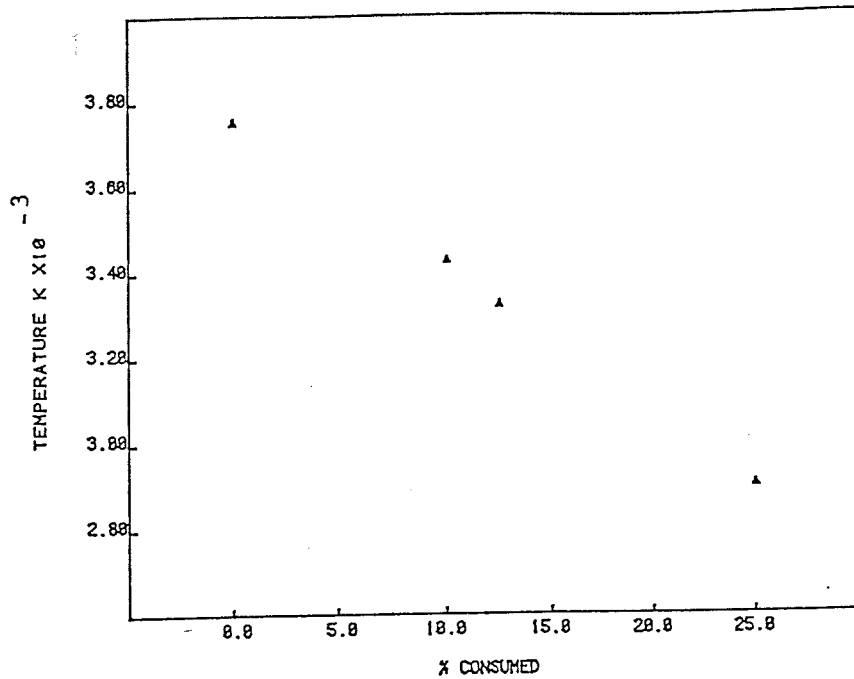


Figure 6. Temperature and % transfer composition consumed  
(Si added)

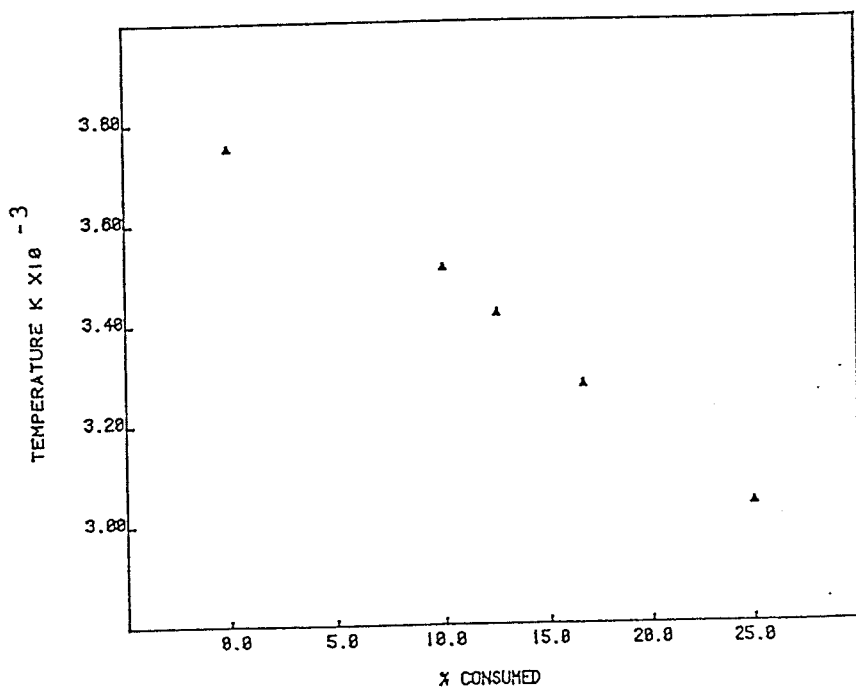


Figure 7. Temperature and % transfer composition consumed  
(CuO added)

Figure 5 where various weight % of transfer mix is included in the process. A considerable lowering of temperature is observed when 25% transfer mix is added. At 25% the temperature is 2900 K. The effect of the addition of silicon to the transfer mix is shown in Figure 6. This figure shows the effect of the addition of the modified transfer mix to the output mix. The effect on flame temperature is marginal in the case of silicon. A very small increase in temperature is calculated. The effect of the addition of cupric oxide to the transfer mix is shown in the same way in Figure 7. The effect is a larger increase in flame temperature. While the effect of the Si and CuO additives appear to be rather marginal as far as equilibrium effects are concerned, the general lowering of the flame temperature by the transfer mix may be significant and serves as a possible mechanism for the observed flame oscillations. Initially, in the course of events, the transfer mix reacts without producing large amounts of gas and produces relatively low temperatures as compared to the output mix. As the output mix burns, higher temperatures are produced. With increasing temperature the transfer mix could well contribute increasingly to the flame process and temperature, and in the process bring the flame temperature down. These alternate processes could explain the observed flame oscillations. Further insight would be obtained with flame temperature measurements and spectroscopic measurements of flame composition.

A second example of this technique was to observe the laser interaction with a high explosive up to the point of ignition. The entire beam, with an average power of 30 watts and a 6 kHz pulse repetition rate, was focused onto a small pellet of the explosive hexanitrostilbene (HNS) for these experiments. There was enough scattered laser light from the focused spot to illuminate the region above the pellet. Figures 8 and 9 show HNS just prior to ignition and just after ignition, respectively. Clouds of explosive vapor or condensable decomposition products were clearly visible above the HNS pellet in Figure 8. When the pellet ignites, it burns with a flame that is above the surface of the pellet, as shown in Figure 9.

A final example of this technique shows two different igniters while they are firing. The experiments were performed to see the effects of different types of closure disks on the devices. The two igniters functioned very differently, which is clearly seen from the films. The closure disk that gave little confinement had very little combustion of the pyrotechnic materials as they exited the device. The closure disk, or pieces of it, could clearly be seen moving away from the device as it functioned. The other component had a closure disk that confined the pyrotechnic material to a greater degree before it ruptured. The effect of this confinement was clear from the films. The pyrotechnic material was burning as it left the device, and there was considerably more self-illumination. Photographs taken from the fifth frame of the high-speed films of the two components are shown in Figures 10 and 11 for comparison. It was very obvious that the increased confinement made the component function more vigorously.

#### CONCLUSION

The value of the copper vapor laser to illuminate and photograph the reactions of energetic materials and components has been demonstrated. The structure of the flames from the components is clearly visible and should be of interest to those persons modeling these reactions. By comparing the laser-illuminated image to the image that is only self-illuminated, information on the character of the flame could be determined. The difference between hot and cold particles, for example, was clearly visible. The calculations performed on the torch have given some insight into the function of this device. Additional insight into the performance of this and similar devices could be obtained with spectroscopic temperature and composition measurements. Similarly, it would be of considerable interest to probe the region directly above the surface of the burning pellet of HNS with laser spectroscopic techniques to determine reactive intermediates important to the combustion.



Figure 8. HNS prior to ignition.



Figure 9. HNS after ignition.  
Left image is laser-illuminated.

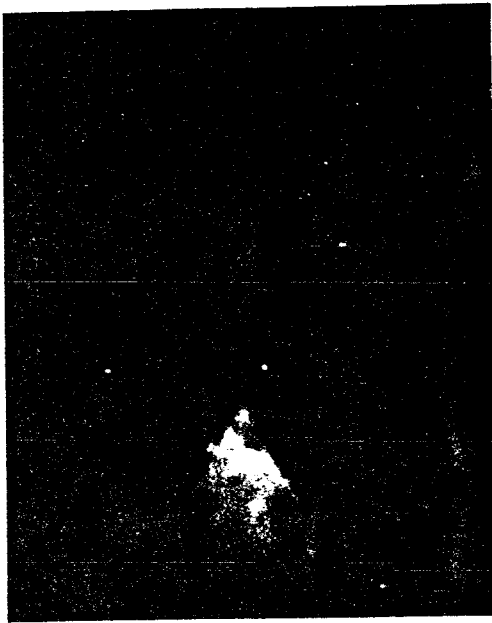


Figure 10. Igniter with closure disk  
that provided little confinement.  
Image is laser-illuminated.

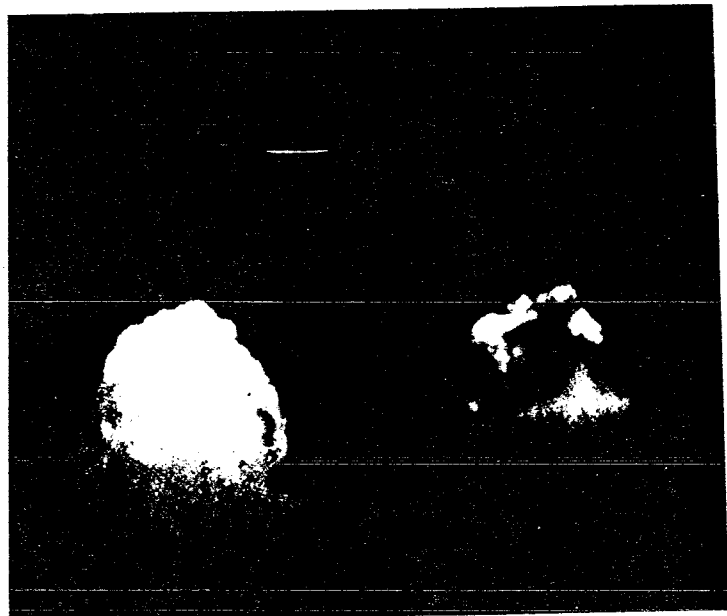


Figure 11. Igniter with closure  
disk that provided a higher  
degree of confinement. Left  
image is laser-illuminated.

Reference

1. S. Gordon and B. J. McBride, "Computer for Calculation of Complex Chemical Equilibrium Compositions, Rocket Performance, Incident and Reflected Shocks, and Chapman-Jouquet Detonations," NASA SP-273, National Aeronautics and Space Administration, Washington, DC, 1971.